Comparison of parallel connected medium voltage grid side VSCs for offshore wind turbines

2015 Tenth International Conference on Ecological Vehicles and Renewable Energies (EVER)

Comparison of Parallel Connected Medium Voltage Grid Side VSCs for Offshore Wind Turbines

Paolo Pescetto
Energy Department
Politecnico di Torino
10129, Torino, Italy
paolo.pescetto91@gmail.com

Gilbert Bergna-Diaz
SINTEF Energy Research
7034, Trondheim, Norway
gilbert.bergna-diaz@sintef.no

Ignacio Zubimendi
Ingeteam Power Technology S.A.
48170, Zamudio, Spain
ignacio.zubimendi@ingeteam.com

Elisabetta Tedeschi
Dep. of Electric Power Eng.
NTNU
7491, Trondheim, Norway,
tedeschi@ieee.org

***Abstract*—The goal of this paper is to compare different solutions for the parallelization of grid side voltage source converters operating in medium voltage for application in multi-megawatt (MW) offshore wind turbines. The study takes into account different alternatives in terms of both topology and modulation: in particular it considers whether the DC busses are common or separated, the output filters are isolated or coupled, and, in the latter case, the impact of the coupling coefficient value. The use of interleaving modulation technique is also analyzed. Systematic comparative analyses are reported with the goal of orienting trade off design choices for offshore converters.**

Keywords— inverter paralelization, grid side converter, output filter, interphase inductance, wind turbine.

I. INTRODUCTION

Offshore wind energy resources are significantly more powerful and constant than onshore ones. They can be exploited with larger wind turbines (WTs), since they are not constrained by road transportation and they imply much less visual and noise impact than onshore installations. All these factors are boosting the offshore energy wind sector and a total of 7.34 GW of installed offshore wind capacity, from more than 2300 wind turbines has been reached in Europe in 2014 [1]. Although best-selling offshore wind turbine are in the range of 3-4 MW, they are rapidly evolving towards much higher power levels. The biggest offshore wind turbine, recently deployed in Denmark is rated 8 MW [2] and larger sizes up to 10 MW are also being proposed [3]. The increasing demand for improved WT control and the stricter requirements set by grid codes are leading to a widespread use of full-power back-to-back power converter solutions. In addition, the need to process power flows in the range of several MW encourages the use of several power converter lines connected in series or in parallel [4] Such modular approach may imply intrinsic system redundancy, allowing the WT to continue operating even in case of a faulted conversion line, thus resulting in higher system reliability. Moreover, the multi-cell approach allows an improvement of the system efficiency by reducing the number of cells used in case of low winds.

Several research activities are ongoing on multi-cell converters for wind power applications, considering both Low Voltage (LV) and Medium Voltage (MV) solutions.

Compared to LV converters, MV solutions reduce the cost of cables and connections and give a further advantage in terms of reliability due to the lower number of components required.

This paper focuses on the parallelization of medium voltage grid side converters for multi-MW wind turbines. It considers and compares in a systematic way the system performance under different configuration and operation scenarios. In particular, it analyses the effect of separated and connected DC busses as well as the type of magnetic coupling (if any) of the output inductance. The impact of the selected PWM strategy, which may or may not imply interleaving, is also considered. For the sake of simplicity, a reference test case based on the standard two-level converter topology is considered, the objective of the paper being the comparison of the different solutions under equal operative conditions and not the definition of an optimized topology.

II. CONSIDERED SYSTEM

In this paper, a multi cell power electronics interface suitable for high power medium voltage off-shore wind turbines is studied. The focus of the work is on the grid side converter of the WT, which is connected to an electric network, operating at a medium voltage level of 3.3kV.

The system under consideration is based on two Voltage Source Converter (VSCs) working in parallel, as illustrated in Figure 1.a-d. In such a figure, multiple configurations are given, depending on whether the DC bus capacitance is common or independent between the converters and based on the coupling of the inductors. The different implications of the configurations are analyzed in detail in the following sections.

In terms of converter control, the possibility of interleaving has been considered in the literature and has proven to be beneficial for the sizing of the filter inductors. As only two converters are considered in this paper, a 180° phase shift between both of the VSCs carrier signals is used for the interleaving implementation, as described in Section V.

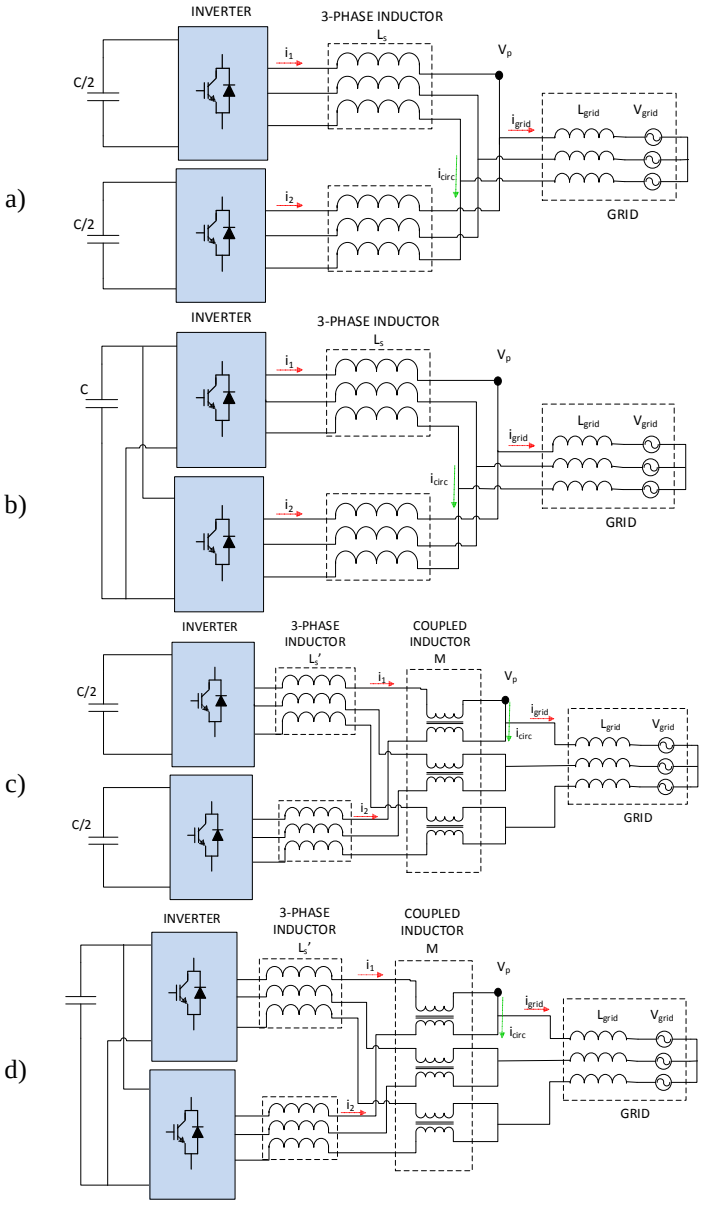

Figure 1 Considered Topologies: a)Separated DC bus, insulated inductor b)Connected DC bus, insulated inductor c)Separated DC bus, coupled inductor d)connected DC bus, coupled inductor

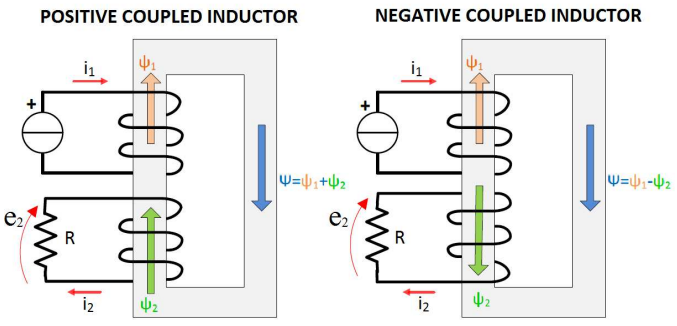

Figure 2 Positive and negative coupled inductor scheme

III. CONNECTED VS SEPARATED BUSSES

The use of the separated DC bus configuration increases the redundancy of the system, which is reduced in common DC bus configurations. By contrast, an advantage of common dc-bus configurations is that both of the inverters have the same instantaneous input voltage. This is particularly beneficial for precise implementation of the interleaving technique, as explained in section V. In addition, when the interleaving technique is utilized in the common DC bus configuration, the THD of the DC bus voltage is also reduced.

By contrast, as the separated DC bus case might lead to differences in the two capacitor voltages, the interleaving may be not perfectly implemented and result in harmonics close to the carrier frequency band. Nonetheless their amplitude is usually significantly lower than if interleaving modulation is not used.

Assuming that the grid topology does not allow zero-sequence current (e.g.: in case of delta connection of the transformers), the existence of such a current component is possible only under the common DC bus configuration. The common capacitor connection offers a path for it to flow, resulting in a *circulating current* between both converters, which does not affect the main grid, but increases the losses in the converter system and affects the system design since all the components must withstand such a current.

A circulating current might appear even if the dc-busses are separated [5], but it can only be formed by positive and/or negative sequence components as there is no path for the zero-sequence in such a case. Thus, assuming equal converter and filter parameters, the circulating current is usually smaller using separated dc-busses [6].

IV. POSSIBLE TYPES OF OUTPUT FILTERS

Several topologies have been proposed in the literature [7] for the converter inductive filter, e.g., it can be insulated or coupled, and the coupling can be positive or negative. In the case of positive coupling the fluxes due to the two converter currents are added in the inductor core, while in the case of negative coupling the fluxes are subtracted, as shown in Figure 2.

The main disadvantage of insulated inductors (Figure 1a-b) is that the current in one of the VSCs does not influence the other; hence, the match between the two currents is regulated only by the inverter control system. In contrast, the use of coupled inductors can provide beneficial effects such as to naturally reduce the circulating current or to limit the output current harmonic content without increasing the size of the filter [8].

In this article, it has been considered that the coupled inductors are implemented as interphase filters; i.e., a filter coupling each phase of the first VSC with the correspondent phase of the second VSC (Figure 1.c-d).

Zhang *et al.* analyzed the effects of a common mode (CM) and an interphase filter in [9]: Unlike common mode filters, interphase inductors can limit both the CM and the differential mode (DM) of the circulating current. Therefore, this solution is usually preferred and has been used in this work.

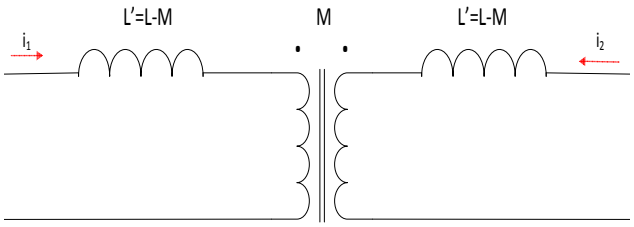

Figure 3 Simplified model of the (positively) coupled inductor.

Interphase filter inductances can present a positive or negative magnetic coupling, as shown in the simplified circuit of Figure 2.

For the sake of clarity, the effect of the coupling sense (positive or negative) on the circulating current is briefly recalled in the following.

For this purpose, the currents in the interphase inductor has been divided as follows:

$$i_1 = i_2 + \Delta i \tag{1}$$

Where i_1 and i_2 are the currents of converter 1 and 2, respectively, for the same corresponding phase, and Δi represents the circulating current, which should be zero under ideal conditions. Assuming that the system behaves linearly, the superposition property can be used by studying independently the contribution of each converter.

The equations of the system for negative coupling are presented below:

$$Ni_1(t) - Ni_2(t) = R\Psi \tag{2}$$

$$e_2(t) = N\frac{\partial \Psi}{\partial t} \tag{3}$$

$$e_2(t) = -ri_2(t) \tag{4}$$

Where *N* is the numbers of windings turns (the same in each circuit), *R* is the reluctance of the circuit, Ψ is the magnetic flux and e_2 the induced voltage on the second winding, having a resistance equal to *r*. Taking the time derivative in both sides of equation (2) and rewriting the flux derivative as a function of i_2 yields:

$$\frac{\partial}{\partial t}\left(i_1(t) - i_2(t)\right) = \frac{R}{N}\frac{\partial \Psi}{\partial t} \tag{5}$$

$$\frac{\partial}{\partial t}\left(i_1(t) - i_2(t)\right) = \frac{R}{N^2}e_2(t) = \frac{1}{L}e_2(t) \tag{6}$$

$$\frac{\partial i_1(t)}{\partial t} = \frac{\partial i_2(t)}{\partial t} - \frac{r}{L}i_2(t) \tag{7}$$

From (7) it is possible to see that the derivatives of both currents have the same sign, meaning that a variation of one of the currents produces a variation of the other current in the same sense. This naturally reduces the circulating current, Δi.

By contrast, positive coupled inductors give the following equations:

$$Ni_1(t) + Ni_2(t) = R\Psi \tag{8}$$

While (3) and (4) still hold. Consequently, the solution is

$$\frac{\partial i_1}{\partial t} = -\frac{\partial i_2}{\partial t} - \frac{r}{L}i_2(t) \tag{9}$$

From (9) the opposite conclusion can be drawn: since the current derivatives have opposite signs, a variation of the current of the first converter is followed by a variation of the other current in the opposite sense. Consequently the circulating current will be amplified.

As a consequence, with negative coupling, if $i_1 = i_2$ the total flux in the inductor will be null, and the filter will have no effect on the total output current. By contrast, with positive coupling, under the same conditions, the flux in the core will be twice as much as the equivalent insulated filter case, increasing the circulating current, but at the same time reducing more efficiently the harmonic components of the output grid current.

V. PWM MODULATION STRATEGY

The literature presents many different Pulse Width Modulation (PWM) techniques. The most classical ones are Sinusoidal PWM (SPWM) and Space Vector Modulation (SVM), but many variations can be used.

Sinusoidal Pulse Width Modulation (SPWM) technique is considered for the inverters in this paper. Even if Discontinuous Space Vector Modulation (D-SVM) can give better performances [10],[11] for the system under study, the aim of this work is to analyze and compare different topologies working under the same control strategy.

Table **1** Nominal values

NOMINAL VALUES		
P_n	9	MW
V_n	3,3	kV
I_n	1,58	kA
f	50	Hz
V_{dc}	5,4	kV
I_{DC_tot}	1,67	kA
C_{tot}	10	mF
L_s	0,11	mH
L_{grid}	0,0011	mH
Coupling coefficient	50	%
Switching frequency	1050	Hz

In particular, VSC interleaving techniques can be used under the parallel converter configuration. This technique consists in a phase shift between the triangular carriers of the two PWM

generators, which has a beneficial effect on the output waveforms. As reported in the literature [12],[13], the phase shift in the carriers causes the cancellation of part of the harmonics, but it increases the mismatch between the systems voltage, increasing the circulating current. For the two parallel VSC case, a phase shift of 180° is usually used, but different phase shift angles are possible. A research of the optimal solution has been carried out following different deductive reasoning by many authors, such as in [14] and [15].

Apart from the possible application of the interleaving techniques, in this work, the same control philosophy has been used for every configuration, in order to analyze the influence of the different topologies independently of the adopted control technique.

VI. SIMULATIONS

A. Simulation model description

In order to simulate the four topologies presented in Figure 1, a corresponding simulation model has been implemented in Matlab/Simulink® and used to carry out the analyses presented in the following. As mentioned earlier, the converter topology is based on a two-level VSC, which has been modeled using the "Universal Bridge" block with ideal switches. The block "Mutual Inductance" with appropriate settings has been used to model both separated inductors and interphase inductors. Regarding the control structure, both parallel converters have the same cascaded control implementation. The internal control loop is based on a standard PI regulator for the current control, whereas the outermost control loop uses another PI regulator to control the DC voltage of the capacitor. In case of common busses a single DC link control loop is implemented, and the output current reference is equally split between the two inner loops regulating the current in the two converters. The main simulation parameters of the selected test case are reported in Table 1.

B. Comparison of the four different topologies

In order to verify the considerations presented above, four different topologies for the grid side converter of a WT have been simulated and compared. The four studied configurations, showed in Figure 1, are:

1. Separated DC-busses with insulated output inductive filters (Figure 1–a),
2. Common DC-bus with insulated output inductive filters (Figure 1–b)
3. Separated DC-busses with partially coupled output inductive filters (Figure 1–c)
4. Common DC-bus with partially coupled output inductive filters (Figure 1–d)

The interphase filter used for the magnetic coupling in cases 3 and 4 has been analyzed with both positive and negative coupling. Moreover, all the configurations have been simulated with and without using the interleaving in order to verify its effects.

For the configurations 1 and 3, half of the capacitance has been used in each bus, and for the inductance in configurations 3 and 4 a coupling of 50% has been used as the base case. As can be inferred from Figure 3, under such condition. $L' = M = L/2 = L_s / 2$. The grid has been simulated as a three-phase voltage source in series with a 3-phase inductance. These parameters have been summarized in Table 1.

For each configuration, the instantaneous DC voltage, V_{DC} , the output currents of each inverter (i_1^{abc} and i_2^{abc}) and the total output AC voltages, v_p^{abc} , and currents, i_{grid}^{abc}) have been considered. From these quantities, the ripple ΔV_{DC} , the zero-sequence current in one VSC i_o , the circulating current i_{circ} and its zero-sequence component i_{circ_0} have been calculated. The results of each system have been compared, Figure 4 shows some of the most relevant waveforms trends obtained using negatively coupled inductors for both configurations; i.e., common DC bus and independent DC bus. By contrast, Figure 5 presents the equivalent waveforms for the positively coupled case. Both figures have been obtained using the nominal 50% coupling coefficient.

According to the theory previously discussed, the zero-sequence current in each VSC is null in every separated bus configuration, while it is present in the common DC bus configuration as in the latter case there is a path for it to flow. This is confirmed by the waveform trends depicted in both Figure 4-a) and Figure 5-a). Despite that zero-sequence current does not exists for the separated DC bus configurations, the positive and negative sequence components are still present, as shown in Figure 4-b) and Figure 5-b). For the common DC bus configuration, the zero-sequence component represents an important percentage of the total circulating current, between 39.7% and 91.7% as given in Table 2. It can be therefore explained why the circulating current in common DC bus configurations tends to be bigger than in case of separated DC busses.

The circulating currents obtained using negatively coupled inductors depicted in Figure 5-a) and b) are significantly smaller than those shown in Figure 4-a) and b) where positively coupled inductors are used instead. This graphical illustration intends to demonstrate the advantage of using negatively coupled inductors in such a system. Nonetheless, the grid current in the positively coupled inductor configuration (given in Figure 4-c) has lower THD than for the case of negatively coupled inductors (shown in Figure 5-c). Moreover, the common DC bus configuration has a positive impact on the THD of the DC bus voltage, as Figure 6 suggests. However, such configuration has the inherent disadvantage of reducing the redundancy of the system.

The effects of the interleaving are also visible from Figure 4-c) and Figure 5-c): it improves the grid current THD due to the harmonic cancellation but it also produces more circulating current due to the higher instantaneous mismatch between the VSCs. Figure 7 and Figure 8 give a broad comparison of the

main features discussed in the present section. More precisely, Figure 7 compares the negatively coupled inductors configurations with their insulated inductors counterpart, in terms of the following parameters:

- DC Voltage Ripple
- Grid current and voltage THD
- % Circulating current
- % Zero-Seq. Circulating current
- Redundancy

Figure 8 shows the equivalent charts for the positively coupled inductor configuration.

In these charts, all the data have been normalized with respect to the configuration that presents the highest value in each analyzed quantity. No redundancy has been considered for configurations with common DC bus, since a fault in the bus will put the all system out of service. Except for the output power, the compared data represent quantities that have to be limited. So, the area inside each line gives an idea of the quality of the correspondent configuration, since a topology can be considered more suitable if it presents smaller values in each section. Thus, smaller area implies better overall performance.

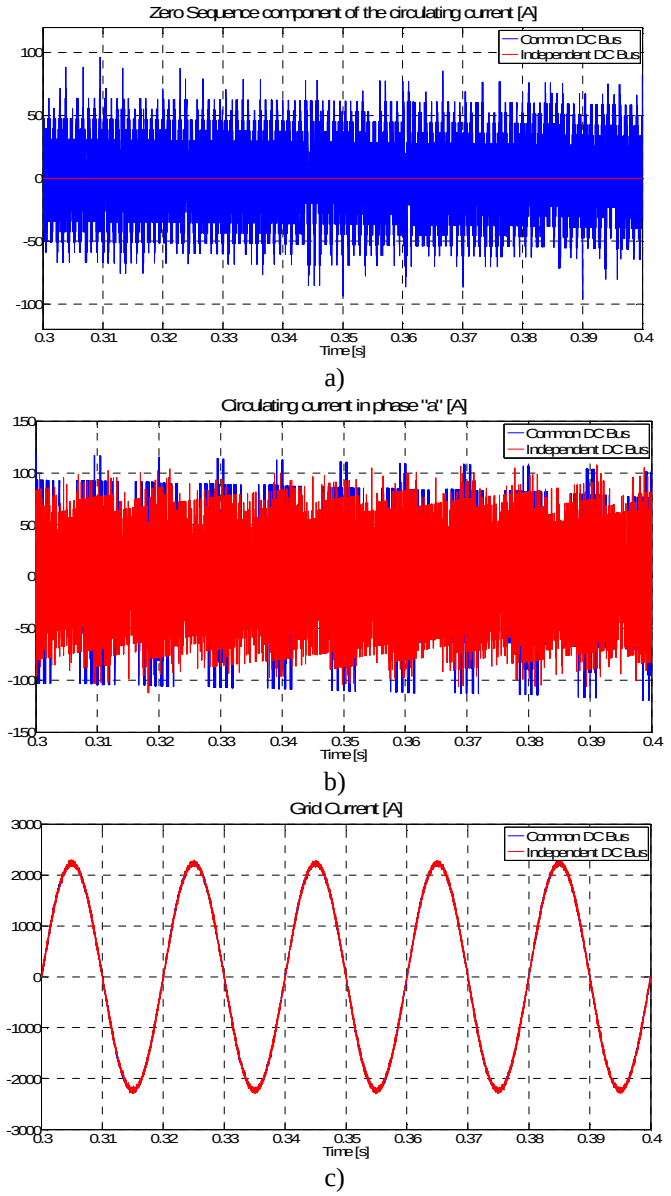

Figure 4 Waveform trends of the *positively* coupled (50%) inductor configuration using interleaving showing both Common (blue) and Independent (red) DC bus configuration: a) Zero-Seq. Circulating Current, b) Circulating current in phase "a," c) grid current.

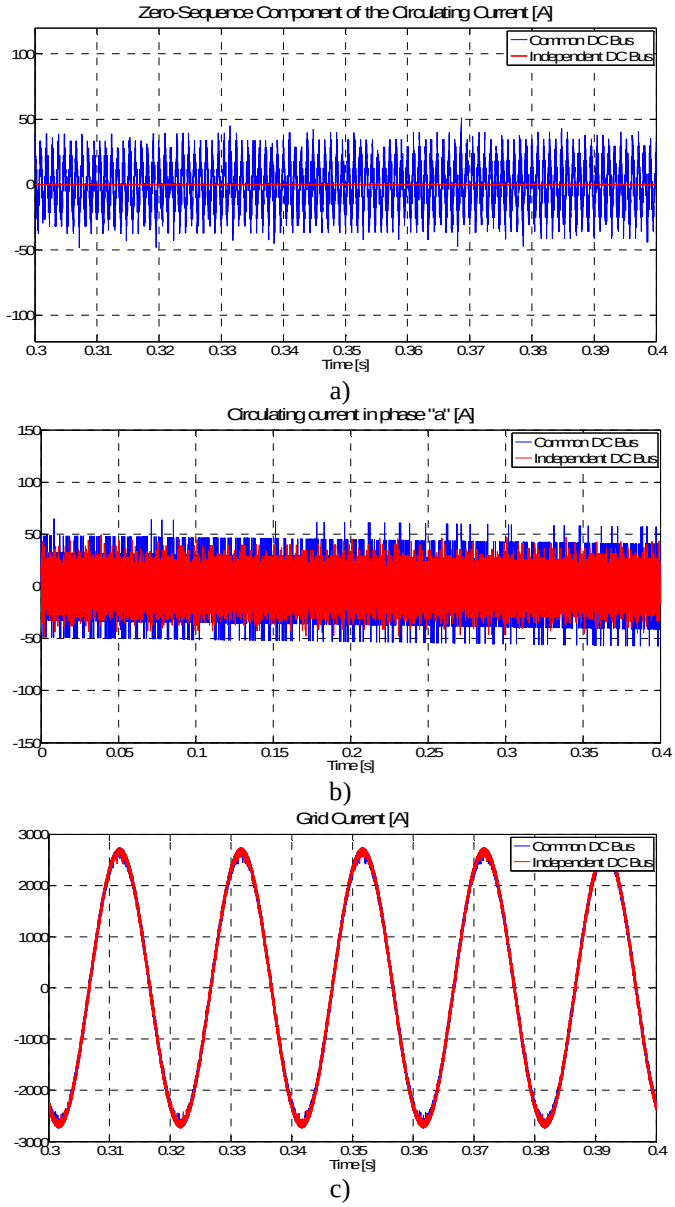

Figure 5 Waveform trends of the *negatively* coupled (50%) inductor configuration using interleaving showing both Common (blue) and Independent (red) DC bus configuration: a) Zero-Seq. Circulating Current, b) Circulating current in phase "a," c) grid current.

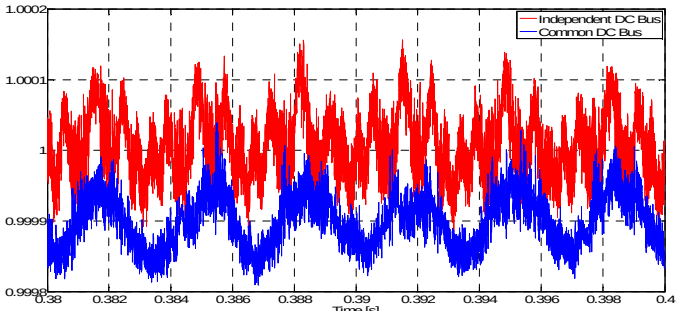

a)

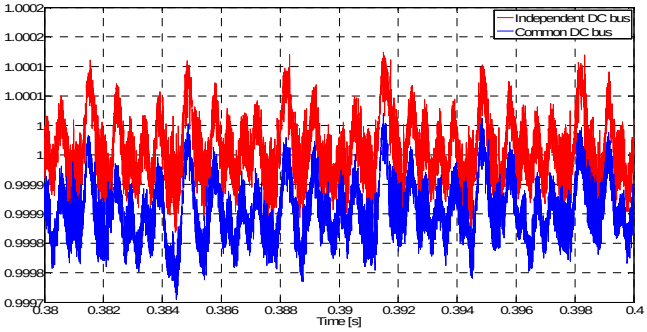

b)

Figure 6 DC bus voltage in p.u.: Common vs. Independent DC bus connection: a) with interleaving, b) without interleaving.

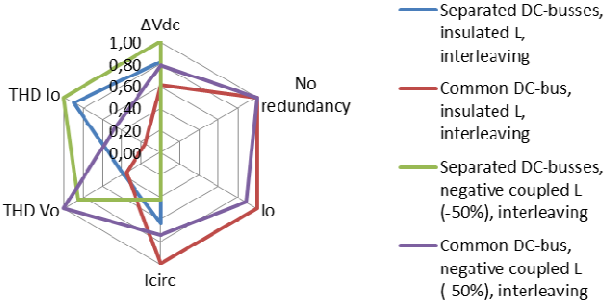

a)

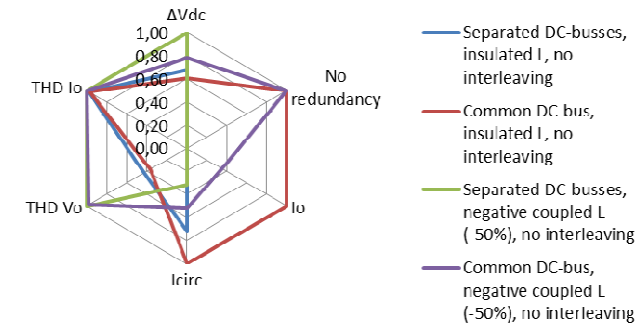

b)

Figure 7 Charts comparing the performance using insulated vs. negatively coupled inductors a) with interleaving and b) without interleaving.

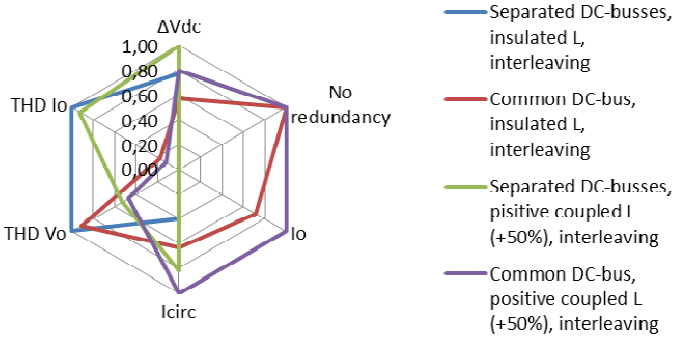

a)

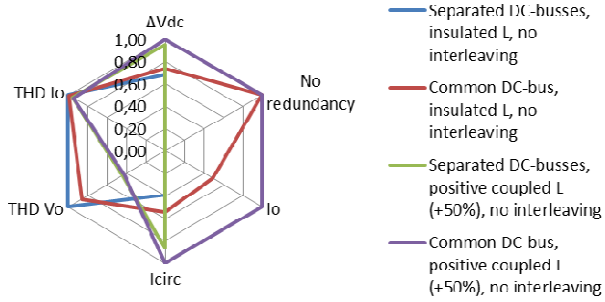

b)

Figure 8 Charts comparing the performance using insulated vs. positively coupled inductors a) with interleaving and b) without interleaving.

C. Parametric effect of the coupling coefficient

The topologies using interphase coupled inductors with common or separated DC busses have been tested varying the coupling coefficient both for positive and negative coupling. Both circuits have been simulated with coupling coefficient between -80% and 80%, with and without the interleaving technique. In each simulation, the value of the total inductance, L_s, has been kept constant. Therefore, while increasing the mutual coupling, the self-inductance of each phase decreases as can be inferred from Figure 3. Results of each simulation are shown in Table 2. As it is possible to see, increasing the module of the coupling coefficient for negative coupled inductors, the circulating current is reduced; whereas for positive coupling, the increase in the coupling coefficient increases the circulating current.

The output current THD is higher in configurations with negatively coupled filters. This is because in such configurations, only the uncoupled part of the inductance contributes as series output filter to reduce the ripple, hence the output harmonic content is bigger. As the coupling coefficient is reduced, the uncoupled part of the filter inductance increases, reducing the THD. On the other hand, the current and voltage THD in configurations with positive coupling inductance tends to be lower than the configurations with insulated filters, as shown in Table 2 and Figure 9. The only cases where this does not occur (for significant values of positive coupling marked with a "*" in Table 2), are due to the fact that in these cases the self-inductance L' becomes so small that in some instants it jeopardizes the performance of the VSC controller.

VII. DISCUSSION

The analysis of the above presented cases confirmed that for the configuration presenting independent DC busses, the zero sequence current does not appear as there is no path for it. However, it is still possible to have a circulating current formed by positive or negative sequence components and must be taken into account as it will contribute to the system efficiency. By contrast, when the configuration considered has a common dc-bus, a zero-sequence current also appears as part of the circulating current. This circulating current is usually larger than the one that appears in the separated dc-busses case.

Regarding the output inductance topology, the negative interphase coupling between the VSCs decreases the circulating current, but increases the output harmonic content; whereas positive coupling of the filter inductors significantly increases the circulating current, but it efficiently reduces its ripple because of the high CM flux in the core. Hence a tradeoff solution should be found at the design stage of the WT converter.

The use of interleaving increases the circulating currents of the system (especially in the case of positively coupling coefficient), but it lowers the harmonic content of the output current. The output harmonic limitation could however be ensured in such cases by the application of multilevel converter topologies, instead of standard 2-level VSC. Since, however, the goal of this paper is not the sizing of the different circuit components, but the comparative analysis of their effect on the system; the specific component choice does not affect the validity of the study, as long as the controllability of the system is ensured.

VIII. CONCLUSIONS

This paper studies the impact of different design and modulation choices on the performance of parallel MV grid side converters used for multi-MW wind turbine applications. Using a simplified test case based on two-level VSCs, the study aims to complement the existing literature on parallel operation of grid connected voltage source converters. This is done by performing a systematic comparative analysis, which considers at the same time I) DC bus interconnection II) output filter topology, III) value of the coupling filter coefficient (if any) and IV) impact of the interleaving modulation technique.

REFERENCES

[1] G. Corbetta, I. Pineda, J. Wilkes., “The European offshore wind industry - key trends and statistics 1st half 2014”, Report of the European Wind Energy Association, July 2014, pp. 1-7

[2] MHI Vestas, “The V164-8.0 MW Turbine”. (available at: http://www.mhivestasoffshore.com/Products-and-services/The-Turbines/V164)

[3] AMSC “SeaTitan™ 10 MW Wind Turbine”, 2012, (available at: www.amsc.com/documents/seatitan-10-mw-wind-turbine-data-sheet/)

[4] Chivite-Zabalza, J.; Larrazabal, I.; Zubimendi, I.; Aurtenetxea, S.; Zabaleta, M., "Multi-megawatt wind turbine converter configurations suitable for off-shore applications, combining 3-L NPC PEBBs," Energy Conversion Congress and Exposition (ECCE), 2013 IEEE , vol., no., pp.2635,2640, 15-19 Sept. 2013

[5] Xiongfei Wang; Blaabjerg, F.; Zhe Chen, "An improved design of virtual output impedance loop for droop-controlled parallel three-phase voltage source inverters," Energy Conversion Congress and Exposition (ECCE), 2012 IEEE , vol., no., pp.2466,2473, 15-20 Sept. 2012

[6] Dongsul Shin; Jong-Pil Lee; Kyoung-Jun Lee; Tae-Jin Kim; Dong-Wook Yoo; Fang Zheng Peng; Baoming Ge; Honnyong Cha, "1.5MVA grid-connected interleaved inverters using coupled inductors for wind power generation system,"Energy Conversion Congress and Exposition (ECCE), 2013 IEEE , vol., no., pp.4689,4696, 15-19 Sept. 2013

[7] Asimmoaei, L.; Aeloiza, E.; Kim, J.H.; Enjeti, P.; Blaabjerg, F.; Moran, L.T.; Sul, S.K., "An interleaved active power filter with reduced size of passive components," Applied Power Electronics Conference and Exposition, 2006. APEC '06. Twenty-First Annual IEEE , vol., no., pp.8 pp.,, 19-23 March 20

[8] Shin, Dongsul; Lee, Kyoung-Jun; Kim, Hee-Je; Lee, Jong-Pil; Kim, Tae-Jin; Yoo, Dong-Wook, "Coupled inductors for parallel operation of interleaved three-phase voltage source grid-connected inverters," Applied Power Electronics Conference and Exposition (APEC), 2013 Twenty-Eighth Annual IEEE , vol., no., pp.2235,2239, 17-21 March 2013

[9] Di Zhang; Fei Wang; Burgos, R.; Boroyevich, D., "Total Flux Minimization Control for Integrated Inter-Phase Inductors in Paralleled, Interleaved Three-Phase Two-Level Voltage-Source Converters With Discontinuous Space-Vector Modulation," Power Electronics, IEEE Transactions on , vol.27, no.4, pp.1679,1688, April 2012

[10] Gohil, G.; Maheshwari, R.; Bede, L.; Kerekes, T.; Teodorescu, R.; Liserre, M.; Blaabjerg, F., "Modified Discontinuous PWM for Size Reduction of the Circulating Current Filter in Parallel Interleaved Converters," Power Electronics, IEEE Trans. on , vol.PP, no.99, pp.1,1

[11] Vafakhah, B.; Knight, A.; Salmon, J., "Reducing losses in multilevel coupled inductor inverters using interleaved discontinuous SVPWM," Applied Power Electronics Conference and Exposition (APEC), 2010, 25th Annual IEEE pp.2013,2020, 21-25 Feb. 2010

[12] Fen Tang; Xinmin Jin; Yibin Tong; Jingdou Liu; Fei Zhou; Lin Ma, "Parallel interleaved grid-connected converters in MW-level wind power generation," Electric Machines and Drives Conference, 2009. IEMDC '09. IEEE International , vol., no., pp.789,796, 3-6 May 2009

[13] Matsui, K.; Asao, M.; Ueda, F.; Tsuboi, K.; Iwata, K., "A technique of parallel-connections of pulsewidth modulated NPC inverters by and using current sharing reactors," Industrial Electronics, Control, and Instrumentation, 1993. Proceedings of the IECON '93., International Conference on , vol., no., pp.1246,1251 vol.2, 15-19 Nov 1993

[14] Prasad, J.S.S.; Narayanan, G., "Minimization of Grid Current Distortion in Parallel-Connected Converters Through Carrier Interleaving," Industrial Electronics, IEEE Transactions on , vol.61, no.1, pp.76,91, Jan. 2014

[15] Anping Hu; Xu, D.; Jianhui Su; Bin Wu, "DC-link current balancing and ripple reduction for direct parallel current-source converters," IECON 2012 - 38th Annual Conference on IEEE Industrial Electronics Society , vol., no., pp.4955,4960, 25-28 Oct. 2012

[16] Yan Jiang; Shan Xiong; Shou Dao Huang; Ke Yuan Huang; Lei Xiao, "Control of circulating current in parallel three-phase inverter in MW wind power system," Electrical Machines and Systems (ICEMS), 2010 International Conference on , vol., no., pp.133,136, 10-13 Oct. 2010.

[17] Cougo, B.; Meynard, T.; Gateau, G., "Parallel Three-Phase Inverters: Optimal PWM Method for Flux Reduction in Intercell Transformers," Power Electronics, IEEE Transactions on , vol.26, no.8, pp.2184,2191, Aug. 2011

[18] Ewanchuk, J.; Salmon, J., "Three-limb Coupled Inductor Operation for Paralleled Multi-level Three-Phase Voltage Sourced Inverters," Industrial Electronics, IEEE Transactions on , vol.60, no.5, pp.1979,1988, May 2013

[19] Abusara, M.A.; Sharkh, S.M., "Design and Control of a Grid-Connected Interleaved Inverter," Power Electronics, IEEE Transactions on , vol.28, no.2, pp.748,764, Feb. 2013

[20] Di Zhang; Wang, F.; Burgos, R.; Rixin Lai; Boroyevich, D., "DC-Link Ripple Current Reduction for Paralleled Three-Phase Voltage-Source Converters With Interleaving," Power Electronics, IEEE Transactions on , vol.26, no.6, pp.1741,1753, June 2011

Table 2 Comparison among the considered test cases

			CONFIGURATIONS WITH SEPARATED DC BUSSES						CONFIGURATIONS WITH COMMON DC BUSSES					
	Coupling %	Interleaving	ΔVdc %	I_0/I_{grid} %	I_{circ}/I_{grid} %	I_{circ_0}/I_{circ} %	THD Vo %	THD Io %	ΔVdc %	I_0/I_{grid} %	I_{circ}/I_{grid} %	I_{circ_0}/I_{circ} %	THD V_o %	THD Io %
NEGATIVE COUPLED INDUCTORS	-80 %	no	0,05	0	0,28	0	7,68	2,01	0,05	0,10	0,26	39,70	7,67	2,01
		yes	0,05	0	0,60	0	6,65	1,50	0,04	0,97	1,06	91,67	7,85	1,39
	-65 %	no	0,04	0	0,30	0	4,51	1,78	0,03	0,26	0,54	48,52	4,48	1,78
		yes	0,03	0	0,63	0	3,88	1,26	0,03	1,02	1,14	89,52	4,60	0,81
	-50 %	no	0,03	0	0,43	0	3,17	1,72	0,03	0,26	0,69	37,21	3,09	1,72
		yes	0,03	0	0,70	0	2,70	1,19	0,02	1,07	1,23	87,03	3,18	0,55
	-35 %	no	0,03	0	0,63	0	2,43	1,70	0,03	0,40	0,89	44,76	2,28	1,70
		yes	0,02	0	0,81	0	2,05	1,14	0,02	1,10	1,30	84,70	2,35	0,39
	-20 %	no	0,02	0	0,74	0	1,85	1,69	0,03	0,46	1,10	41,51	1,88	1,70
		yes	0,02	0	0,89	0	1,62	1,11	0,02	1,12	1,42	79,09	1,85	0,30
SEP AR.	0 %	no	0,02	0	0,96	0	1,35	1,68	0,02	0,73	1,34	54,20	1,16	1,67
		yes	0,02	0	1,06	0	1,22	1,07	0,02	1,20	1,66	72,25	1,11	0,19
POSITIVE COUPLED INDUCTORS	20 %	no	0,03	0	1,34	0	0,82	1,65	0,02	0,95	1,58	60,10	0,74	1,64
		yes	0,02	0	1,36	0	0,90	1,04	0,02	1,41	1,94	72,89	0,74	0,13
	35 %	no	0,03	0	1,64	0	0,69	1,63	0,03	1,13	1,90	59,78	0,64	1,62
		yes	0,02	0	1,67	0	0,76	1,02	0,02	1,45	2,21	65,32	0,63	0,12
	50 %	no	0,03	0	2,12	0	0,59	1,60	0,03	1,48	2,46	60,32	0,57	1,59
		yes	0,03	0	2,14	0	0,64	0,99	0,02	1,68	2,62	64,38	0,57	0,13*
	65 %	no	0,04	0	3,03	0	0,52	1,55	0,04	2,19	3,64	60,24	0,51	1,53
		yes	0,04	0	3,15	0	0,55	0,95	0,03	2,37	4,31	55,12	0,51	0,15*
	80 %	no	0,06	0	5,38	0	0,47	1,47	0,06	3,59	6,54	54,93	0,47	1,43
		yes	0,06	0	5,42	0	0,49	0,86	0,06	3,68	6,48	56,81	0,46	0,24*

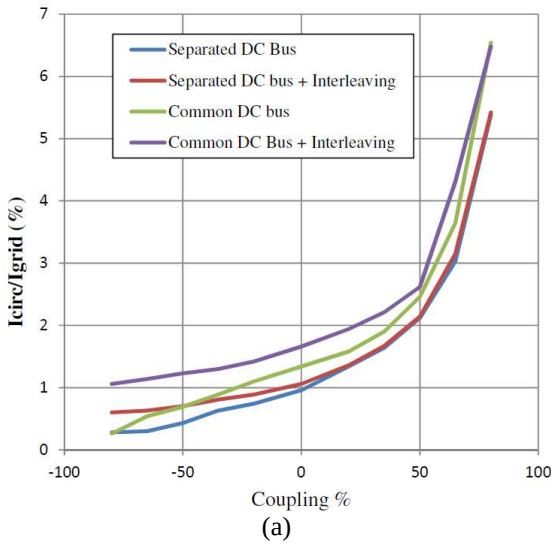

(a)

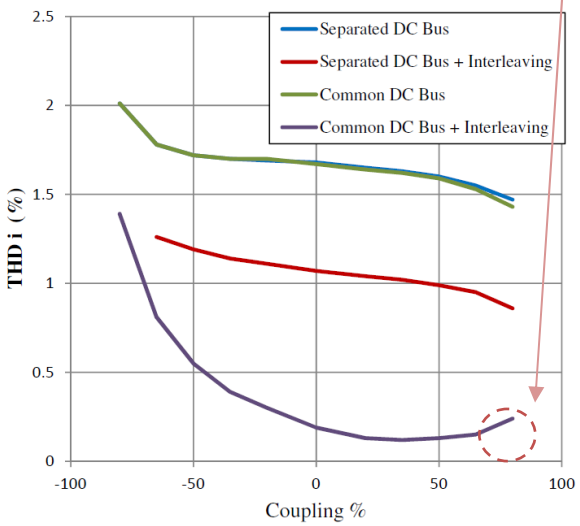

(b)

Figure 9 Comparison between Common DC Bus and Independent DC Bus with and without interleaving in terms of a) I_{circ}/I_{grid} % and b) THDi %.